specific. This result furthers our understanding of both the clinical and allelic heterogeneity displayed in Japanese DEB patients.

Acknowledgements The authors wish to thank Akari Nagasaki and Megumi Sato for technical assistance and Dr. James R. McMillan for proofreading and comments concerning this manuscript. This work was supported in part by a Grant-In-Aid for Scientific Research from the Japanese Society for the Promotion of Science (15390337 to D.S., 13357008 to H.S., and 15390336 to H.S.) and by a Health and Labor Sciences Research Grant (Research on Measures for Intractable Diseases to H.S.). Informed consent both for the research and for publication of the photographs was obtained from the families in this study. We thank the patients and their families for their interest in our study. We thank the referring physicians at Kyushu University, Nara Medical University, Asahikawa Medical College, National Hospital Organization Okayama Medical Center, Shimada Municipal Hospital, the University of Yamanashi, Kakogawa Municipal Hospital, Kanazawa Medical University, and Osaka Red Cross Hospital for providing clinical information on the patients.

References

Christiano AM, Morricone A, Paradisi M, Angelo C, Mazzanti C, Cavalieri R, Uitto J (1995) A glycine-to-arginine substitution in the triple-helical domain of type VII collagen in a family with dominant dystrophic epidermolysis bullosa. J Invest Dermatol 104:438–440

Christiano AM, Hoffman GG, Zhang X, Xu Y, Tamai Y, Greenspan DS, Uitto J (1997) Strategy for identification of sequence variants in *COL7A1*, and a novel 2 bp deletion mutation in recessive dystrophic epidermolysis bullosa. Hum Mutat 10:408–414

Fine JD, Eady RA, Bauer EA, Briggaman RA, Bruckner-Tuderman L, Christiano A, Heagerty A, Hintner H, Jonkman MF, McGrath J, McGuire J, Moshell A, Shimizu H, Tadini G, Uitto J (2000) Revised classification system for inherited epidermolysis bullosa: report of the Second International Consensus Meeting on diagnosis and classification of epidermolysis bullosa. J Am Acad Dermatol 42:1051–1066

Gardella R, Castiglia D, Posteraro P, Bernardini S, Zoppi N, Paradisi M, Tadini G, Barlati S, McGrath JA, Zambruno G, Colombi M (2002) Genotype-phenotype correlation in Italian patients with dystrophic epidermolysis bullosa. J Invest Dermatol 119:1456–1462

Jarvikallio A, Pulkkinen L, Uitto J (1997) Molecular basis of dystrophic epidermolysis bullosa: mutations in the type VII collagen gene (*COL7A1*). Hum Mutat 10:338–347

Jonkman MF, Moreno G, Rouan F, Oranje AP, Pulkkinen L, Uitto J (1999) Dominant dystrophic epidermolysis bullosa (Pasini) caused by a novel glycine substitution mutation in the type VII collagen gene (*COL7A1*). J Invest Dermatol 112:815–817

Kon A, Nomura K, Pulkkinen L, Sawamura D, Hashimoto I, Uitto J (1997) Novel glycine substitution mutations in *COL7A1* reveal that the Pasini and Cockayne–Touraine variants of dominant dystrophic epidermolysis bullosa are allelic. J Invest Dermatol 109:684–687

Lee JY, Li C, Chao SC, Pulkkinen L, Uitto J (2000) A de novo glycine substitution mutation in the collagenous domain of *COL7A1* in dominant dystrophic epidermolysis bullosa. Arch Dermatol Res 292:159–163

Mellerio JE, Dunnill MGS, Allison W, Ashton GH, Christiano AM, Uitto J, Eady RA, McGrath JA (1997) Recurrent mutations in the type VII collagen gene (*COL7A1*) in patients with recessive dystrophic epidermolysis bullosa. J Invest Dermatol 109:246–249

Murata T, Masunaga T, Ishiko A, Shimizu H, Nishikawa T (2004) Differences in recurrent *COL7A1* mutations in dystrophic epidermolysis bullosa: ethnic-specific and worldwide recurrent mutations. Arch Dermatol Res 10:442–447

Pulkkinen L, Uitto J (1999) Mutation analysis and molecular genetics of epidermolysis bullosa. Matrix Biol 18:29–42

Rouan F, Pulkkinen L, Jonkman MF, Bauer JW, Cserhalmi-Friedman PB, Christiano AM, Uitto J (1998) Novel and de novo glycine substitution mutations in the type VII collagen gene (*COL7A1*) in dystrophic epidermolysis bullosa: implications for genetic counseling. J Invest Dermatol 116:1210–1213

Salas-Alanis JC, Amaya-Guerra M, McGrath JA (2000) The molecular basis of dystrophic epidermolysis bullosa in Mexico. Int J Dermatol 39:436–442

Sato-Matsumura KC, Yasukawa K, Tomita Y, Shimizu H (2002) Toenail dystrophy with COL7A1 glycine substitution mutations segregates as an autosomal dominant trait in 2 families with dystrophic epidermolysis bullosa. Arch Dermatol 138:269–271

Sato-Matsumura KC, Sawamura D, Goto M, Goto M, Nakamura H, Shimizu H (2003) A novel insertion mutation in COL7A1 identified in Hallopeau-Siemens recessive dystrophic epidermolysis bullosa. Acta Derm Venereol 83:137–138

Shimizu H, McGrath JA, Christiano AM, Nishikawa T, Uitto J (1996) Molecular basis of recessive dystrophic epidermolysis bullosa: genotype/phenotype correlation in a case of moderate clinical severity. J Invest Dermatol 106:119–124

Tamai K, Murai T, Mayama M, Kon A, Nomura K, Sawamura D, Hanada K, Hashimoto I, Shimizu H, Masunaga T, Nishikawa T, Mitsuhashi Y, Ishida-Yamamoto A, Ikeda S, Ogawa H, McGrath JA, Pulkkinen L, Uitto J (1999) Recurrent *COL7A1* mutations in Japanese patients with dystrophic epidermolysis bullosa: positional effects of premature termination codon mutations on clinical severity. J Invest Dermatol 112:991–993

Tomita Y, Sato-Matsumura KC, Sawamura D, Matsumura T, Shimizu H (2003) Simultaneous occurrence of three squamous cell carcinomas in a recessive dystrophic epidermolysis bullosa patient. Acta Derm Venereol 83:225–226

Uitto J, Hovnanian A, Christiano AM (1995) Premature termination codon mutations in the type VII collagen gene (*COL7A1*) underlie severe recessive dystrophic epidermolysis bullosa. Proc Assoc Am Phys 107:245–252

Whittock NV, Ashton GH, Mohammedi R, Mellerio JE, Mathew CG, Abbs SJ, Eady RA, McGrath JA (1999) Comparative mutation detection screening of the type VII collagen gene (*COL7A1*) using the protein truncation test, fluorescent chemical cleavage of mismatch, and conformation sensitive gel electrophoresis. J Invest Dermatol 113:673–686

DOI 10.1111/j.1365-2133.2005.06778.x

Prenatal exclusion of harlequin ichthyosis; potential pitfalls in the timing of the fetal skin biopsy

A. Shimizu, M. Akiyama,* A. Ishiko, T. Yoshiike,† K. Suzumori‡ and H. Shimizu*

Department of Dermatology, Keio University School of Medicine, Tokyo, Japan
*Department of Dermatology, Hokkaido University Graduate School of Medicine, N15 W7, Kita-ku, Sapporo 060-8638, Japan
†Department of Dermatology, Juntendo University Izu-Nagaoka Hospital, Shizuoka, Japan
‡Department of Obstetrics and Gynaecology, Nagoya City University School of Medicine, Nagoya, Japan

Correspondence
Masashi Akiyama, M.D. Ph.D.
E-mail: akiyama@med.hokudai.ac.jp

Accepted for publication
26 February 2005

Key words:
electron microscopy, hair follicle, hair peg, harlequin fetus, lamellar granule, skin development

Conflicts of interest:
None declared.

Summary

Background Harlequin ichthyosis (HI) is a severe and usually fatal congenital skin disorder with autosomal recessive inheritance. Several cases of HI prenatal diagnosis have been performed using fetal skin biopsy, mainly at around 23 weeks estimated gestational age (EGA), and reported in the literature. However, prenatal testing must be done earlier than 21 weeks EGA in several countries including Japan where the present HI families live, because termination is legally allowed only until 22 weeks EGA.

Objectives We report the successful prenatal exclusion of HI in two fetuses from two independent families and discuss the technical difficulties and potential pitfalls in the prenatal exclusion of HI at early gestation stages.

Methods Fetal skin biopsy specimens and amniotic fluid samples at 19 and 20 weeks EGA from two fetuses at risk of HI were examined by light and electron microscopy.

Results For the prenatal diagnosis in case 1, the fetal skin biopsy samples were obtained at 20 weeks EGA and showed normal keratinization in the hair canals; no abnormalities were observed in the keratinized cells. In case 2, the interfollicular epidermis and the hair follicles in the samples obtained at 19 weeks EGA had not differentiated enough to show proper keratinization. However, lamellar granules were normally formed in the inner root sheath cells of the late bulbous hair pegs. From these ultrastructural findings, the case 1 fetus was diagnosed as unaffected with HI, and the case 2 fetus was diagnosed as unlikely to be affected. Subsequently, both were born as healthy, unaffected babies.

Conclusions The timing of biopsies at 19 weeks EGA is not ideal for fetal skin biopsy because the samples are not always sufficiently differentiated for the prenatal diagnosis of HI. However, morphological observations of lamellar granules gives us important additional information useful for HI prenatal diagnosis.

Harlequin ichthyosis (HI) (MIM 242500) is an extremely severe and usually fatal hereditary skin disorder with an autosomal recessive inheritance.[1] The characteristic clinical features of HI include thick, plate-like scales over the entire body with ectropion, eclabium and flattened ears.[2] Fetal skin biopsy has been performed for prenatal testing for this severe genodermatosis. In the affected fetus, skin development in the later stages is markedly altered *in utero*; hyperkeratosis of the hair canal occurs in the second trimester and the characteristic ultrastructural abnormalities are expressed after 22–23 weeks estimated gestational age (EGA).[3–7] Prenatal testing must be done earlier than 21 weeks EGA in several countries, including Japan, because termination is legally allowed only until 22 weeks EGA.

Here, we report the prenatal exclusion of HI in two fetuses from two independent families using ultrastructural examination of fetal skin biopsy specimens and amniotic fluid at 19 and 20 weeks EGA, and discuss the technical difficulties and potential pitfalls of HI prenatal exclusion at early gestation stages.

Materials and methods

Case 1

The proband was the second child of healthy Japanese parents and was born at 29 weeks and 3 days of pregnancy by Caesarean section performed for pre-eclampsia. The

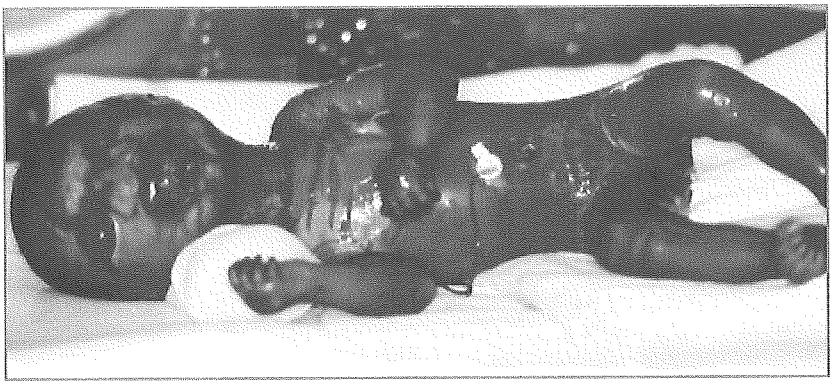

Fig 1. Clinical features of the proband of the case 1 family. The entire body was covered in thick plate-like hyperkeratosis and severe ectropion and eclabium were seen on the face.

proband's clinical features were typical of HI (Fig. 1). The proband died at the age of 8 days. There was no family history of any genodermatosis or consanguinity within the family. One year after the death of the first child, the mother became pregnant again and the parents requested a prenatal diagnosis.

Case 2

The proband was the first child of healthy Japanese parents and was born at 30 weeks and 5 days of pregnancy. During the second pregnancy, a prenatal diagnosis was performed and the pregnancy was terminated at the parents' request after a positive prenatal diagnosis. Details of the proband and the second pregnancy were previously reported.[7–9] Five years after the termination of the second child, the mother became pregnant for the third time and the parents requested prenatal diagnosis again.

Fetal skin biopsy and amniotic fluid sampling

After thorough genetic counselling and explanation of the sensitivity, specificity and the risks of HI prenatal testing, fetal skin biopsies were performed at 20 and 19 weeks' gestation in the first and second cases, respectively. Several skin samples, approximately 1 mm^3 in size, were obtained and there were no complications from the procedure in either case. One aliquot (≈5 mL) of amniotic fluid was obtained from each case just prior to fetal skin biopsy and these were processed for the morphological analysis of amniotic fluid cells. Each sample was prepared for light and electron microscopy as previously described.[10]

Results

The skin morphology of the affected newborns (probands)

Proband of the case 1 family

Light microscopic observation showed a remarkable hyperkeratosis and hypergranulosis (Fig. 2a). At the ultrastructural level, a large number of vacuoles, lipid droplets and dense bodies were observed in the horny layer cells (data not shown). In the granular layer keratinocytes, a large number of abnormal lamellar granules were also observed (Fig. 2b). According to the classification reported by Dale *et al.*,[4] the proband could be classified as HI type I.

Proband of case 2 family

Details of the morphological observations of the proband of case 2 family, corresponding to HI type 1, were previously reported.[8]

Morphological features of fetal skin biopsy specimens at 19–20 weeks' gestation

Case 1 (fetal skin biopsy at 20 weeks' gestation)

At the light microscopic level, the interfollicular epidermis failed to show complete cornification. Only the hair canals showed keratinization, but no apparent abnormalities were identified (Fig. 2c). At the electron microscopic level, abnormal lipid vacuoles were not observed in the cytoplasm of the cornified cells in the hair canal (data not shown). Normal-shaped lamellar granules were seen (Fig. 2d).

Case 2 (fetal skin biopsy at 19 weeks' gestation)

The entire epidermis showed no apparent abnormalities at the light microscopic level. The interfollicular epidermis failed to show cornification and was still covered with the periderm (Fig. 3a). Bulbous hair pegs were seen, but no follicular keratinization was observed in any of the biopsy specimens (Fig. 3b). Careful electron microscopic observation at high magnification showed normal-shaped lamellar granules at the periphery of the upper layer follicular keratinocytes in the intraepidermal portion of the bulbous hair pegs (Fig. 3c).

Morphological observation of amniotic fluid cells

In the amniotic fluid cell pellets, several cell aggregates were observed and no abnormalities were observed at the light

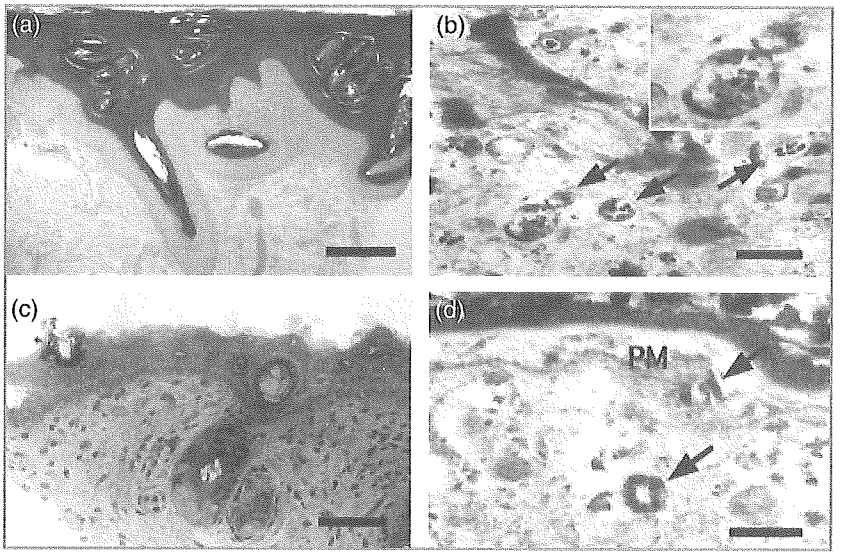

Fig 2. Morphological features of the proband (a,b) and the case 1 fetus (c,d) in case 1 family. (a) Light microscopic observation of semithin sections in a skin specimen from the back of the proband shows marked hyperkeratosis of the epidermis extending to the hair follicle. Hair canals were widely opened and filled with keratin plugs. (b) High magnification electron microscopic view of the proband showed the abnormal shape of lamellar granules (arrows) in the granular cell layer. Inset: abnormal lamellar granules containing many abnormal vesicles and particles. (c) A fetal skin biopsy sample, which was obtained at 20 weeks' gestation, showed no apparent abnormality. The interfollicular epidermis showed no cornification and was still covered with the periderm. Keratinization was seen only in the hair canals without any abnormalities. (d) High magnification electron microscopic view of the fetal skin biopsy sample showed normal lamellar granules (arrows) in the granular cells. One lamellar granule was secreting its lamellar contents into the intercellular space. PM, Plasma membrane. Bars: a, 1 mm, b and d, 200 nm, c, 500 μm.

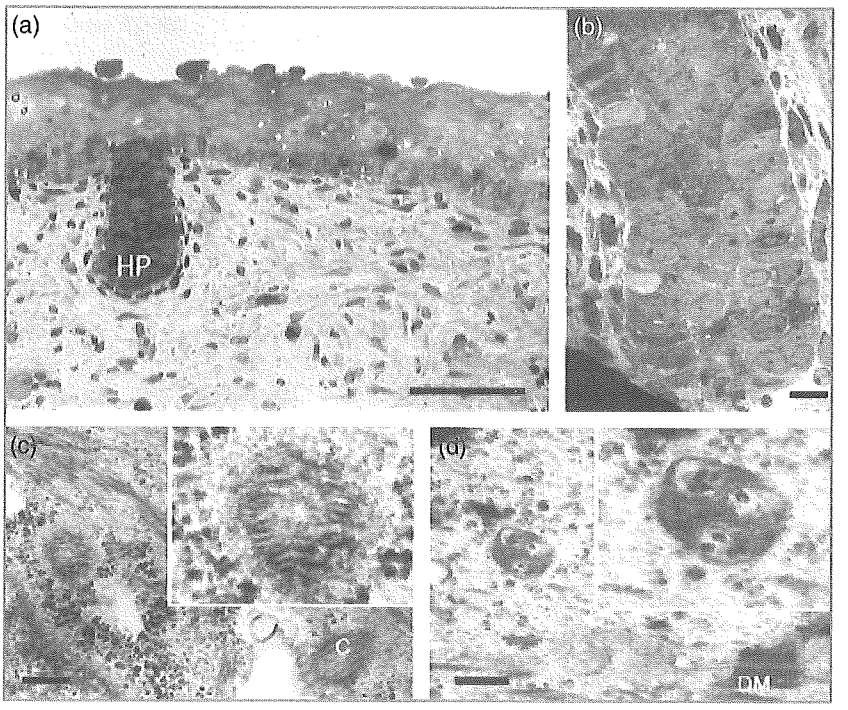

Fig 3. Morphological features of case 2 fetus (a–c) and the proband (d) in case 2 family. (a) Light microscopic observation of a 19 weeks' gestation fetal skin biopsy sample showed that the epidermis was still covered by periderm and did not show any keratinization in the interfollicular epidermis. HP, Hair peg. (b) By electron microscopy, no sign of keratinization was confirmed in any part of the hair peg of the fetal skin biopsy sample. (c) In this sample, normal lamellar granules were seen in follicular cells in the intraepidermal portion of a bulbous hair peg. Inset: a lamellar granule with normal lamellar contents. c, Centrosome. (d) Conversely, the lamellar granules of the proband showed an apparent abnormality. Inset: the lamellar granules contained small particles in the centre of the vesicle. DM, Desmosome. Bars: a, 500 μm, b, 10 μm, c and d, 200 nm.

microscopic level. Electron microscopic observation revealed that these pellets contained several normal-shaped keratinized cells. The cytoplasm comprised electron-dense amorphous or filamentous material (data not shown).

Prenatal exclusion and outcome

From the ultrastructural findings from fetal skin specimens and amniotic fluid samples, the fetus from the case 1 family

was diagnosed as unaffected with HI. In the fetus from the case 2 family, we reported that there was no evidence of the fetus being affected, although HI could not be completely excluded. Subsequently, the mothers in both families gave birth to healthy males.

Discussion

Previously, several cases of successful prenatal diagnoses of HI have been performed based upon the examination of fetal skin biopsy samples obtained between 19 and 23 weeks' gestation[5,9,11] and of amniotic fluid at 17 weeks EGA.[10] According to these reports, fetal skin biopsy specimens at 19–23 weeks EGA showed the characteristic abnormalities that were sufficient for the correct prenatal detection of the disorder. The interfollicular epidermis at 19 weeks EGA has not sufficiently differentiated to exhibit the characteristic morphological features of keratinization.[12] However, hair canals, where keratinization is known to occur much earlier at around 15 weeks EGA in human fetal skin development,[13] reveal the characteristic changes of HI in affected fetuses by 19 weeks' gestation. In fact, in the prenatal diagnosis in case 1, the fetal skin biopsy samples showed normal keratinization in the hair canals and we could exclude HI in this fetus with relatively high confidence.

On the other hand, it was more difficult to exclude HI from the findings in the case 2 fetal skin biopsy samples, which were obtained at 19 weeks EGA. This was because the hair follicles in the samples had not sufficiently differentiated. We could not identify any keratinized cells even after careful observation in any of these specimens. The lamellar granules were normally formed, without any abnormalities in their size and shape, in the inner root sheath cells of the late bulbous hair pegs. These findings pointed to the fact that these fetuses were unaffected, even if we could not directly confirm normal keratinization. Terminal hair development is more advanced in the scalp than that seen in vellus hair regions, such as the trunk or limbs.[12,13] Thus, fetal skin biopsy samples taken from the scalp would be better for the detection of aberrant keratinization in HI. However, it is more difficult and risky to take a skin biopsy from the scalp than from the trunk or limbs, and this could not always be recommended.

In conclusion, the morphological observation of lamellar granules can give us useful and important information for prenatal diagnosis. However, we think that findings obtained at around 19 weeks EGA are not always sufficient for the prenatal diagnosis of HI and that the optimum biopsy timing should be after 19 weeks EGA.

Acknowledgments

The authors thank Dr James R. McMillan for the critical reading of this manuscript. This work was supported in part by a Grant-in-Aid from the Ministry of Education, Science, Sports, and Culture of Japan (Kiban B, no. 16390312 to M.A.).

References

1 Akiyama M. The pathogenesis of severe congenital ichthyosis of the neonate. *J Dermatol Sci* 1999; **21**:96–104.
2 Williams ML, Elias PM. Genetically transmitted, generalized disorders of cornification. The ichthyoses. *Dermatol Clin* 1987; **5**:155–78.
3 Blanchet-Bardon C, Dumez Y, Labbe F *et al.* Prenatal diagnosis of a harlequin fetus using electron microscopy. *Ann Pathol* 1983; **3**:321–5.
4 Dale BA, Holbrook KA, Fleckman P *et al.* Heterogeneity in harlequin ichthyosis, an inborn error of epidermal keratinization: variable morphology and structural protein expression and a defect in lamellar granules. *J Invest Dermatol* 1990; **94**:6–18.
5 Suzumori K, Kanzaki T. Prenatal diagnosis of harlequin ichthyosis by fetal skin biopsy; report of two cases. *Prenat Diagn* 1991; **11**:451–7.
6 Akiyama M, Holbrook KA. Analysis of skin-derived amniotic fluid cells in the second trimester; detection of severe genodermatoses expressed in the fetal period. *J Invest Dermatol* 1994; **103**:674–7.
7 Akiyama M, Dale BA, Smith LT *et al.* Regional difference in expression of characteristic abnormality of harlequin ichthyosis in affected fetuses. *Prenat Diagn* 1998; **18**:425–36.
8 Akiyama M, Yoneda K, Kim SY *et al.* Cornified cell envelope proteins and keratins are normally distributed in harlequin ichthyosis. *J Cutan Pathol* 1996; **23**:571–5.
9 Akiyama M, Suzumori K, Shimizu H. Prenatal diagnosis of harlequin ichthyosis by the examination of keratinized hair canals and amniotic fluid cells at 19 weeks' estimated gestational age. *Prenat Diagn* 1999; **19**:167–71.
10 Akiyama M, Kim KD, Main DM *et al.* Characteristic morphologic abnormality of harlequin ichthyosis detected in amniotic fluid cells. *J Invest Dermatol* 1994; **102**:210–13.
11 Blanchet-Bardon C, Dumez Y, Labbe F *et al.* Prenatal diagnosis of Harlequin fetus [letter]. *Lancet* 1983; **15**:132.
12 Holbrook KA, Odland GF. Regional development of the human epidermis in the first trimester embryo and the second trimester fetus (ages related to the timing of amniocentesis and fetal biopsy). *J Invest Dermatol* 1980; **74**:161–8.
13 Holbrook KA, Odland GF. Structure of the human fetal hair canal and initial hair eruption. *J Invest Dermatol* 1978; **71**:385–90.

Experimental Dermatology 2005: 14: 819–823
Blackwell Munksgaard . Printed in Singapore

EXPERIMENTAL DERMATOLOGY
ISSN 0906-6705

Expression of macrophage migration inhibitory factor in rat skin during embryonic development

Shimizu T, Ogata A, Honda A, Nishihira J, Watanabe H, Abe R, Zhao Y, Shimizu H. Expression of macrophage migration inhibitory factor in rat skin during embryonic development.
Exp Dermatol 2005: 14: 819–823. © Blackwell Munksgaard, 2005

Abstract: We have previously shown that human epidermal keratinocytes express macrophage migration inhibitory factor (MIF) mRNA, and immunohistochemical studies showed that MIF is expressed in human epidermis. To explore the possible pathophysiological roles of MIF in skin during rat fetal development, we examined the expression patterns of MIF during rat epidermal development using Northern blot analysis and *in situ* hybridization. Expression of MIF mRNA was first detected by *in situ* hybridization in the developing epidermis and hair germ cells from embryonic day (ED) 16. From ED 19, moderate levels of MIF expression were detected in the epidermis and epithelial sheath cells of growing hair follicles. In postnatal rat skin, higher MIF expression was detected in the epidermis and hair follicles on postnatal day 3. These observations were also confirmed by Northern blot analysis. Immunohistochemical analysis with an anti-MIF antibody showed a similar distribution to that of the mRNA. Our results suggest that MIF is associated with epidermal and hair follicle development.

Tadamichi Shimizu[1], Akihiko Ogata[2], Ayumi Honda[1], Jun Nishihira[3], Hirokazu Watanabe[1], Riichiro Abe[1], Yunan Zhao[1] and Hiroshi Shimizu[1]

[1]Department of Dermatology, Hokkaido University Graduate School of Medicine, Sapporo, Japan;
[2]Department of Neurology, Hokkaido University Graduate School of Medicine, Sapporo, Japan;
[3]GeneticLab Co., Ltd. Sapporo, Japan

Key words: development – *in situ* hybridization – macrophage migration inhibitory factor – rat

Tadamichi Shimizu
Departments of Dermatology
Hokkaido University Graduate School of Medicine
Sapporo 060-8638
Japan
Tel.: +81 11 716 1161x5962
Fax: +81 11 706 7820
e-mail: michiki@med.hokudai.ac.jp

Accepted for publication 13 July 2005

Introduction

Macrophage migration inhibitory factor (MIF), which was originally identified as a lymphokine attractant for macrophages at inflammatory loci, is a potent activator of macrophages and is thought to play an important role in cell-mediated immunity (1). MIF was reportedly mainly expressed in T lymphocytes and macrophages; however, current studies revealed that this protein is ubiquitously expressed in various cells (2,3). Recently, it was reported that endotoxin treatment affects the expression of MIF protein and mRNA in various rat tissues (4). To date, MIF responses to stimuli such as wounding and infection are thought to contribute to the regulation of inflammatory and immunological tissue repair (1,4). In a previous study, we have shown using reverse transcription-polymerase chain reaction analysis that human epidermal keratinocytes express MIF mRNA, and our immunohistochemical studies showed that MIF is expressed in the human epidermis, especially within the basal layer (5). Although the pathophysiological function(s) of MIF in skin remains ambiguous, the fact that MIF is produced by keratinocytes points to a likely biological relevance in cutaneous inflammatory responses and cell growth and differentiation. To explore the possible pathophysiological roles of MIF in skin, we have examined the expression of MIF mRNA during rat fetal development using Northern blot analysis and *in situ* hybridization.

Abbreviations: ED, embryonic days; MIF, macrophage migration inhibitory factor; PD, postnatal days.

Materials and methods

Animals

Fischer rats, used in this study, were purchased from Nippon Clea (Shizuoka, Japan). Embryos were obtained from

pregnant rats at embryonic days (ED) 13, 16, and 19. They were rinsed briefly with 4% paraformaldehyde in 0.1 M phosphate buffer (PB) (pH 7.4) and fixed in the same solution at 4°C overnight. In addition, postnatal day (PD) 3 rats were used. Under ether anesthesia, they were perfused with 4% paraformaldehyde in 0.1 M PB (pH 7.4) and then fixed with solution at 4°C overnight.

Northern blot analysis

Total cellular RNA was isolated from the skin (epidermis plus dermis) of rats at ED 16, 19, and PD 3 using an Isogen extraction kit (Nippon Gene, Toyama, Japan) according to the manufacturer's protocols. Northern blot analysis was carried out as previously described (6). In brief, RNA (20 mg) was separated by electrophoresis on agarose gels containing 0.6 M formaldehyde and blotted onto nylon membrane filters. Hybridization was carried out with a rat MIF cDNA probe, radiolabeled with [α-^{32}P]dCTP by use of a random primer labeling kit. The hybridization was performed in a solution containing the radiolabeled rat MIF cDNA probe, 50% formamide, 0.75 M NaCl, 0.1% sodium dodecyl sulfate (SDS), 20 mM Tris-HCl (pH 7.5), 2.5 mM ethylenediaminetetraacetic acid (EDTA), 0.5× Denhardt's solution (1× Denhardt's solution: 2.5 mM EDTA, 0.5× albumin, 0.2% polyvinylpyrolidone, 0.2% Ficoll), and 10% dextran sulfate at 42°C overnight. After hybridization, the filters were washed with 0.2× standard saline citrate (SSC) (1× SSC: 0.15 M NaCl, 0.015 M sodium citrate), 0.1% SDS at 65°C and subjected to autoradiographic analysis. As a control, the filters were probed with radiolabeled glyceraldehyde-3-phosphate dehydrogenase (GAPDH). Hybridization signals were digitized and quantified with MCID Image Analyzer (Fuji Film, Tokyo, Japan). The density of MIF bands was normalized by the intensities of GAPDH.

In situ hybridization

A Digoxigenin (DIG)-labeled RNA probe complementary to the rat MIF mRNA was prepared using DIG RNA labeling kit (Boehringer Mannheim, St. Louis, MO, USA) as previously described (7). To prepare the template DNA for the rat MIF probe, the full-length sequence was subcloned into pBluescript SK(–) plasmid. This plasmid was either linearized with EcoRI and transcribed with T7 RNA polymerase to prepare an antisense probe or linearized with Hind III and transcribed with T3 RNA polymerase to prepare a sense probe. Using this probe, hybridization was carried out as previously described by Hirota et al. (8). In brief, slides (the skin of rats at ED 13, 16, 19, and PD 3) were hydrated and digested with 10 μg/ml protease K (Sigma, Tokyo, Japan) after deparaffinization. They were fixed with 4% paraformaldehyde in 0.1 M PB. Then, they were treated with 0.2 M HCl to inactivate endogenous alkaline phosphatase and were acetylated by 0.25% acetic anhydride in 0.1 M triethanolamine (pH 8.0). Following dehydration under air, they were incubated in hybridization buffer at 50°C overnight in a moistened chamber. The hybridization solution contained 50% deionized formamide, 10 mM Tris-HCl (pH 7.6), 200 μg/ml tRNA, 1× Denhardt's solution, 10% dextran sulfate, 600 mM NaCl, 1 mM EDTA pH 8.0, and 1 μg/ml of the RNA probe. Following this, slides were washed with 5× SSC(1× SSC: 0.15 M NaCl, 0.015 M sodium citrate) and then with 2× SSC, 50% formamide at 50°C. After the treatment with RNase A, the sections were blocked with a 1% blocking reagent (Boehringer Mannheim) and treated with anti-DIG antibody conjugated with alkaline phosphatase diluted to 1:500 (Boehringer Mannheim) at room temperature for 1 h. Nitroblue tetrazolium chloride and 5-bromo-4chloro-3-indolyl phosphate were used to visualize any positive signal. As a negative control, hybridization was also performed using a sense probe.

Immunohistochemistry

A polyclonal anti-rat MIF antibody was generated by immunizing New Zealand white rabbits with purified recombinant rat MIF as described previously (6). Rat skin of 13, 16, and 19 ED, and PD 3 was embedded in Tissue-Tek OCT Compound and snap frozen in liquid nitrogen and stored at −80°C. The frozen, embedded tissues were cut into 4-μm sections which were collected to slides and fixed in acetone for 10 min at room temperature. They were stained using an avidin–biotin peroxidase complex procedure using a Vector ABC Kit according to the manufacturer's protocol. In brief, the sections were incubated overnight at 4°C with the anti-rat MIF antibody (1:500 dilution). After three washes with phosphate-buffered saline (PBS), the samples were treated with biotinylated goat anti-rabbit immunoglobulin G (IgG) (Cell Signaling Technology, Inc., Beverly, MA, USA)(10 μg/ml) in PBS containing 1% bovine serum albumin and 0.05% NaN_3 for 30 min at 37°C. The slides were washed three times with PBS and were incubated with peroxidase-conjugated streptavidin (100 μg/ml) in PBS at room temperature for 30 min. The reaction was developed in 3,3′-diaminobenzidine tetrahydrochloride containing hydrogen peroxide (0.01%), and the tissue samples were mounted in alkylacrylate. Non-immune rabbit IgG was used as a negative control.

Results

Mild expression of MIF mRNA was first detected at ED 16 in the developing epidermis and developing hair germs (Fig. 1a). Mesenchymal cells in the dermis also expressed MIF mRNA. ED 13 samples failed to show MIF mRNA expression in the developing epidermis (data not shown). From ED 19 onwards, moderate MIF mRNA-expression levels were detected in the developing epidermis and epithelial hair follicle sheath cells (Fig. 1b,c). Sense RNA probes (negative control) showed no MIF mRNA expression in the epidermis (Fig. 1d). Immunohistochemical analysis with anti-MIF antibody at ED 13 failed to show staining in developing skin (data not shown). At ED 16, the anti-MIF antibody showed weak staining in the developing epidermis (Fig. 1e) and moderate staining in the epidermis and hair follicles at ED 19 (Fig. 1f). Non-immune IgG (negative control) failed to show any skin staining at ED 19 (Fig. 1g). In rat skin at PD 3, high expression of MIF mRNA was detected in the epidermis (Fig. 2a), and consistent expression was detected in the hair follicles (Fig. 3b). Immunohistochemical analysis with anti-MIF antibody at PD 3 showed a similar distribution to that seen in the *in situ* hybridization analysis (Fig. 2c). Northern blot analysis showed that MIF mRNA could be faintly detected in ED 16 skin (Fig. 3). MIF mRNA was up-regulated by ED 19 and was clearly detected in PD 3 skin (Fig. 3). Table 1 summarizes the MIF mRNA expression patterns in developing rat skin.

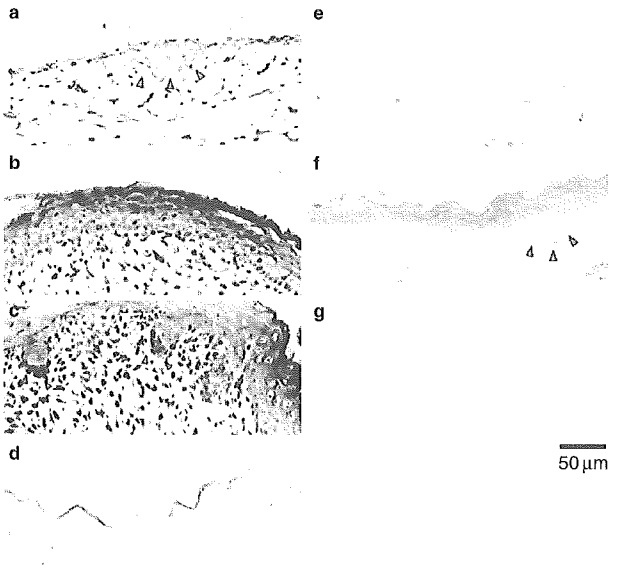

Figure 1. Expression of macrophage migration inhibitory factor (MIF) mRNA and protein in the embryonic stage. *In situ* hybridization using Digoxigenin (DIG)-labeled antisense MIF RNA probe on rat embryo skin sections. On embryonic day (ED) 16, MIF mRNA was first detected in the developing epidermis and hair germs (arrow head) (a). Mesenchymal cells in the dermis also expressed MIF mRNA. On ED 19, the mRNA signal was moderate in both the epidermis (b) and the hair follicles (arrow head) (c). Negative control sections incubated with the DIG-labeled sense MIF RNA probe failed to show any staining in skin at ED 19 (d). An immunohistochemical study using ED 16 rat skin with the anti-MIF polyclonal antibody showed less MIF staining in the developing epidermis (e). At ED 19, MIF was moderately stained in the epidermis and hair follicles (arrow head) (f). Non-immune immunoglobulin G showed no skin staining at ED 19 (g). Bar = 50 μm.

Discussion

MIF was the first lymphokine reported to prevent the random migration of macrophages and recruit them to inflammatory loci (9). MIF has long been considered as exclusively expressed in activated T lymphocytes; however, it is now clear that a variety of cells and tissues have the potential to produce this immunoregulatory protein. From these findings, novel immunological and hormonal MIF functions have been reported including those in the skin (10). Bernhagen et al. (11) reported that the administration of neutralizing anti-MIF antibodies in mice significantly inhibited the development of delayed-type hypersensitivity reactions, affirming the central role of MIF in the immunological response. MIF also counteracts the anti-inflammatory actions of the glucocorticoids (12) and plays an essential role in T-cell activation (13). Recently, we have identified the involvement of MIF in cutaneous wound healing (14,15). We found that MIF is critical for cutaneous inflammatory reactions and immune responses in the defense against ultraviolet B exposure (16). The two MIF-related protein of the S100 family are also expressed in epithelial cells under inflammatory conditions (17). These findings together suggest that MIF plays a critical role in skin inflammation and immunity.

The present study is the first report describing the expression of MIF during skin development. It is known that the epidermis is simple in its structure before ED 13.5 in the rat and that the embryonic epidermis becomes stratified after ED 16 (18). MIF mRNA expression was first detected in the developing epidermis at ED 16, indicating that MIF may be important for epidermal development. High MIF mRNA-expression levels were also detected in mesenchymal cells in the dermis at ED 16 and 19. It has been reported that ED 16 mesenchymal cells are able to induce greater numbers of hair bulbs than ED 14

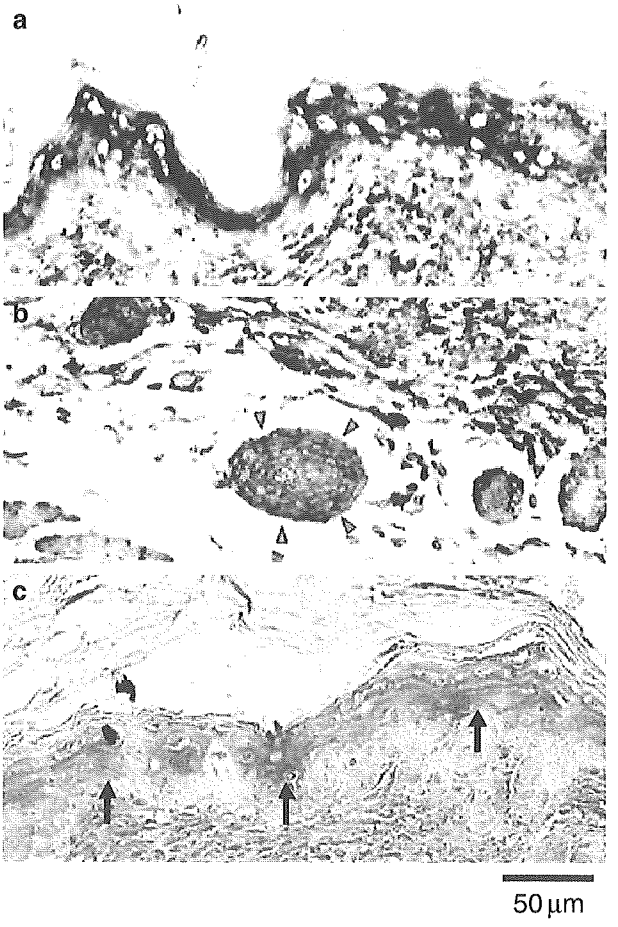

Figure 2. Expression of macrophage migration inhibitory factor (MIF) mRNA and protein in postnatal rat skin. At postnatal day (PD) 3, MIF mRNA signal was strikingly expressed in the epidermis of the skin (a). The MIF mRNA signals were also highly expressed in hair follicles (arrow head) (b). An immunohistochemical study using PD 3 rat skin with the anti-MIF polyclonal antibody showed a similar distribution in the epidermis to that of the *in situ* hybridization (arrow indicate the epidermal basal layer) (c). Bar = 50 μm.

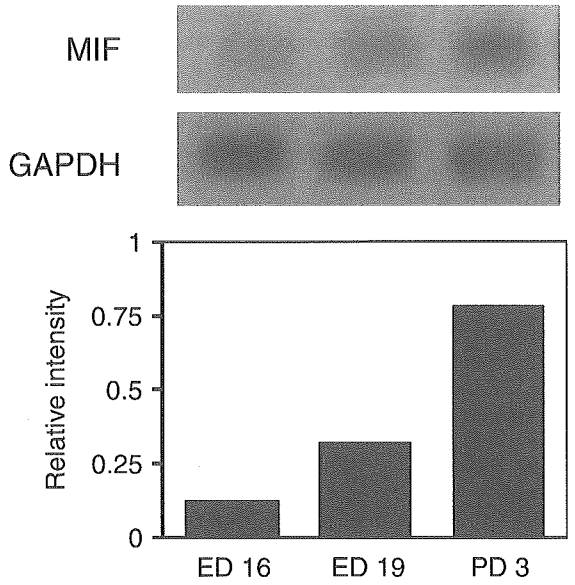

Figure 3. Northern blot analysis of macrophage migration inhibitory factor (MIF) mRNA in embryonic day (ED) 16, 19, and postnatal day (PD) 3 skin. Whole skin (epidermis plus dermis) was subjected to Northern blot analysis as described in the *Materials and methods* section. The densities of MIF bands were normalized to the glyceraldehyde-3-phosphate dehydrogenase (GAPDH) signals. MIF mRNA was first detected on ED 16 skin. MIF mRNA was markedly up-regulated on PD 3 skin.

mesenchymal cells (19). These observations are consistent with the timing of MIF mRNA expression and support the idea that MIF is also involved in the generation of dermal cells such as dermal papilla cells which are able to induce hair follicle progression and development (20). In the present study, MIF mRNA expression levels were detected in the hair germ at ED 16 at the start of hair bud formation.

MIF is expressed in highly proliferative tissues such as the corneal epithelium (21), osteoblasts (22), leukemia cells (23), and the early embryonic chicken lens (24). Expression of MIF in rat brain during fetal development was examined using *in situ* hybridization (7). It is hypothesized that MIF expression may be involved in the generation of both neurons and glial cells (7). Besides the central nervous system, MIF may play an important role in the development of the chicken lens in the eye, where MIF mRNA expression correlates with differentiation of lens cells (24). Moreover, MIF mRNA was also expressed in ovulated ooctyes, zygotes, the two-cell embryo, eight-cell embryo stages, and blastocysts (25). Conversely, targeted disruption of the MIF gene in mice causes no detectable developmental abnormalities (26,27). However, morpholino oligomer-mediated knockdown of MIF caused a severely altered phenotype, which demonstrated that MIF is an essential factor in Xenopus embryogenesis, and suggested the importance of mammalian MIF in the development of mammals (28). A detailed MIF expression pattern during mouse embryogenesis was also reported (29). The report suggests the involvement of MIF in the development of various tissues, although skin development was not proposed (29). Although the precise molecular function of MIF in skin development remains to be elucidated, these findings support the general idea that significant MIF expression may be directly or indirectly associated with the development of epidermis and hair follicles.

Table 1. Summary of macrophage migration inhibitory factor mRNA expression in developing rat skin

Stage	Epidermis	Hair follicle
ED 13	–	–
ED 16	+	–
ED 19	+	+
PD 3	++	++

–, negative; +, positive; ++, strongly positive; ED, embryonic day; PD, postnatal day.

Acknowledgements

This research was supported by a Grant-in-Aid for research (No. 11670813 and 13357008) from the Ministry of Education, Science, and Culture of Japan. We thank Dr James R. McMillan for proofreading this manuscript.

References

1. Calandra T, Bernhagen J, Mitchell R A, Bucala R. The macrophage is an important and previously unrecognized source of macrophage migration inhibitory factor. J Exp Med 1994: 179: 1895–1902.
2. Lanahan A, Williams J B, Sanders L K, Nathans D. Growth factor-induced delayed early response genes. Mol Cell Biol 1992: 12: 3919–3929.
3. Imamura K, Nishihira J, Suzuki M et al. Identification and immunohistochemical localization of macrophage migration inhibitory factor in human kidney. Biochem Mol Biol Int 1996: 40: 1233–1242.
4. Bernhagen J, Calandra T, Mitchell R A et al. MIF is a pituitary-derived cytokine that potentiates lethal endotoxaemia. Nature 1993: 365: 756–759.
5. Shimizu T, Ohkawara A, Nishihira J, Sakamoto W. Identification of macrophage migration inhibitory factor (MIF) in human skin and its immunohistochemical localization. FEBS Lett 1996: 381: 188–202.
6. Suzuki T, Ogata A, Tashiro K et al. A method for detection of a cytokine and its mRNA in the central nervous system of the developing rat. Brain Res Brain Res Protoc 1999: 4: 271–279.
7. Suzuki T, Ogata A, Tashiro K, Nagashima K, Tamura M, Nishihira J. Augmented expression of macrophage migration inhibitory factor (MIF) in the telencephalon of the developing rat brain. Brain Res 1999: 16: 457–462.

8. Hirota S, Ito A, Morii E et al. Localization of mRNA for c-kit receptor and its ligand in the brain of adult rats: an analysis using in site hybridization histochemistry. Brain Res Mol Brain Res 1992: 15: 47–54.
9. Bloom B R, Bennett B. Mechanism of a reaction in vitro associated with delayed-type hypersensitivity. Science 1966: 153: 80–82.
10. Shimizu T. Role of macrophage migration inhibitory factor (MIF) in the skin. J Dermatol Sci 2005: 37: 65–73.
11. Bernhagen J, Bacher M, Calandra T et al. An essential role for macrophage migration inhibitory factor in the tuberculin delayed-type hypersensitivity reaction. J Exp Med 1996: 183: 277–282.
12. Calandra T, Bernhagen J, Metz C N et al. MIF as a glucocorticoid-induced modulator of cytokine production. Nature 1995: 377: 68–71.
13. Bacher M, Metz C N, Calandra T et al. An essential regulatory role for macrophage migration inhibitory factor in T-cell activation. Proc Natl Acad Sci USA 1996: 93: 7849–7854.
14. Abe R, Shimizu T, Ohkawara A, Nishihira J. Enhancement of macrophage migration inhibitory factor (MIF) expression in injured epidermis and cultured fibroblasts. Biochim Biophys Acta 2000: 1500: 1–9.
15. Shimizu T, Nishihira J, Watanabe H et al. Macrophage migration inhibitory factor (MIF) is induced by thrombin and factor Xa in endothelial cells. J Biol Chem 2004: 279: 13729–13737.
16. Shimizu T, Abe R, Ohkawara A, Nishihira J. Ultraviolet B radiation up-regulates the production of macrophage migration inhibitory factor (MIF) in human epidermal keratinocytes. J Invest Dermatol 1999: 112: 210–215.
17. Leukert N, Sorg C, Roth J. Molecular basis of the complex formation between the two calcium-binding proteins S100A8 (MRP8) and S100A9 (MRP14). Biol Chem 2005: 386: 429–434.
18. Oomizu S, Sahuc F, Asahina K et al. Kdap, a novel gene associated with the stratification of the epithelium. Gene 2000: 256: 19–27.
19. Osada A, Kobayashi K. Appearance of hair follicle-inducible mesenchymal cells in the rat embryo. Dev Growth Differ 2000: 42: 19–27.
20. O'Shaughnessy R F, Christiano A M, Jahoda C A. The role of BMP signalling in the control of ID3 expression in the hair follicle. Exp Dermatol 2004: 13: 621–629.
21. Matsuda A, Tagawa Y, Matsuda H, Nishihira J. Expression of macrophage migration inhibitory factor in corneal wound healing in rats. Invest Ophthalmol Vis Sci 1997: 38: 1555–1562.
22. Onodera S, Suzuki K, Matsuno T, Kaneda K, Kuriyama T, Nishihira J. Identification of macrophage migration inhibitory factor in murine neonatal calvariae and osteoblasts. Immunology 1996: 89: 430–435.
23. Nishihira J, Koyama Y, Mizue Y. Identification of macrophage migration inhibitory factor in human leukemia HL-60 cells and its induction by lipopolysaccharide. Biochem Mol Biol Int 1996: 40: 861–869.
24. Wistow G J, Shaughnessy M P, Lee D C, Hodin J, Zelenka P S. A macrophage migration inhibitory factor is expressed in the differentiating cells of the eye lens. Proc Natl Acad Sci USA 1993: 90: 1272–1275.
25. Suzuki H, Kanagawa H, Nishihira J. Evidence for the presence of macrophage migration inhibitory factor in murine reproductive organs and early embryos. Immunol Lett 1996: 51: 141–147.
26. Bozza M, Satoskar A R, Lin G et al. Targeted disruption of migration inhibitory factor gene reveals its critical role in sepsis. J Exp Med 1999: 189: 341–346.
27. Honma N, Koseki H, Akasaka T et al. Deficiency of the macrophage migration inhibitory factor gene has no significant effect on endotoxaemia. Immunology 2000: 100: 84–90.
28. Suzuki M, Takamura Y, Maeno M et al. Xenopus laevis macrophage migration inhibitory factor is essential for axis formation and neural development. J Biol Chem 2004: 279: 21406–21414.
29. Kobayashi S, Satomura K, Levsky J M et al. Expression pattern of macrophage migration inhibitory factor during embryogenesis. Mech Dev 1999: 84: 153–156.

Mutation Analysis of the *ADAR1* Gene in Dyschromatosis Symmetrica Hereditaria and Genetic Differentiation from both Dyschromatosis Universalis Hereditaria and Acropigmentatio Reticularis

Noriyuki Suzuki,* Tamio Suzuki,* Katsuhiko Inagaki,* Shiro Ito,* Michihiro Kono,* Kazuyoshi Fukai,† Hiromichi Takama,‡ Kenji Sato,§ Osamu Ishikawa,¶ Masatoshi Abe,¶ Hiroshi Shimizu,# Masaaki Kawai,** Tatsuya Horikawa,†† Kunihiro Yoshida,‡‡ Kazuhiko Matsumoto,§§ Tadashi Terui,¶¶ Kaoru Tsujioka,## and Yasushi Tomita*

*Department of Dermatology, Nagoya University Graduate School of Medicine, Nagoya, Japan; †Department of Dermatology, Osaka City University Graduate School of Medicine, Osaka, Japan; ‡Takama Dermatology Clinic, Kasugai, Aichi, Japan; §Department of Dermatology, Kinki Central Hospital, Itami, Japan; ¶Department of Dermatology, Gunma University Graduate School of Medicine, Maebashi, Japan; #Department of Dermatology, Hokkaido University Graduate School of Medicine, Sapporo, Japan; **Department of Dermatology, Juntendo University Urayasu Hospital, Urayasu, Japan; ††Department of Dermatology, Kobe University Graduate School of Medicine, Kobe, Japan; ‡‡Division of Clinical and Molecular Genetics, Shinshu University Hospital, Matsumoto, Japan; §§Clinical Trial Research Center, Shinshu University Hospital, Matsumoto, Japan; ¶¶Department of Dermatology, Tohoku University Graduate School of Medicine, Sendai, Japan; ##Department of Dermatology, Japanese Red Cross Society Wakayama Medical Center, Wakayama, Japan

Dyschromatosis symmetrica hereditaria (DSH) (also called "reticulate acropigmentation of Dohi") is a pigmentary genodermatosis of autosomal dominant inheritance. We have clarified for the first time four pathological mutations of the double-stranded RNA-specific adenosine deaminase gene (*ADAR1 or DSRAD*) in four DSH pedigrees. In this paper, we report 16 novel mutations containing six missense substitutions (p.V906F, p.K1003R, p.G1007R, p.C1036S, p.S1064F, p.R1078C), two splice site mutations (IVS2 + 2T > G, IVS8 + 2T > A), six frameshift mutations (p.H216fs, p.K433fs, p.G507fs, p.P727fs, p.V955fs, p.K1201fs), and two nonsense mutations (p.R426X, p.Q600X) found in Japanese patients with DSH. We did not establish any clear correlation between the clinical phenotypes and the genotypes of *ADAR1* gene mutations in our examination of 16 cases plus four pedigrees. None of the different mutations identified in our studies of 20 cases suggested any founder effect. Furthermore, we did not identify any mutations in the *ADAR1* gene of three patients with dyschromatosis universalis hereditaria or three patients with acropigmentatio reticularis, indicating that the two diseases are completely different from DSH, although they have sometimes been suggested to be phenotypical variations of DSH.

Key words: adenosine deaminase/DSRAD/Japanese/pigmentation disorders/RNA editing
J Invest Dermatol 124:1186–1192, 2005

Dyschromatosis symmetrica hereditaria (DSH [MIM127400]) (also called "reticulate acropigmentation of Dohi") is an autosomal dominant disease characterized by a mixture of hyperpigmented and hypopigmented macules distributed on the dorsal aspects of the extremities and freckle-like macules on the face (Toyama, 1910, 1929) (Fig 1*A* and *B*). DSH has been reported mainly in Japan, although a few cases were described among Koreans, Indians, Chinese, Europeans, and South Americans (Oyama *et al*, 1999). Recently, 17 DSH families including 136 cases in China were reported (He *et al*, 2004), indicating that this disorder might be distributed mainly in East Asia. The difference in the frequency of this disorder between East Asia and other regions may be related to genetic background and/or environment, e.g., the amount of UV exposure. From the results of linkage analysis and a genome-wide scan, we have for the first time clarified that a heterozygous mutation of the RNA-specific adenosine deaminase gene (*ADAR1*, *DSRAD*) causes DSH, and have also reported four heterozygous mutations of p.R474X, p.L923P, p.K952X, and p.F1165S in the *ADAR1* gene responsible for DSH in Japanese families (Miyamura *et al*, 2003). Subsequently, two groups reported two and eight novel mutations in the *ADAR1* gene in Chinese patients with DSH, respectively (Li *et al*, 2004; Liu *et al*, 2004; Zhang *et al*, 2004), which confirmed that the *ADAR1* gene is responsible for DSH not only in Japanese but also in another ethnic groups.

ADAR1 was identified as the first enzyme that converts adenosine to inosine in double-stranded RNA (Bass and Weintraub, 1988). Inosine acts as guanosine during translation and reverse-transcription. It appears to be the most widespread type of nuclear pre-mRNA editing in higher eukaryotes. RNA editing reactions occur in many organisms and operate by different molecular mechanisms. In some

Abbreviations: ADAR, adenosine deaminase acting on RNA; AR, acropigmentatio reticularis; DSH, dyschromatosis symmetrica hereditaria; DSRAD, double-stranded RNA-specific adenosine deaminase; DUH, dyschromatosis universalis hereditaria; SSCP/HD, single-strand conformation polymorphism/heteroduplex

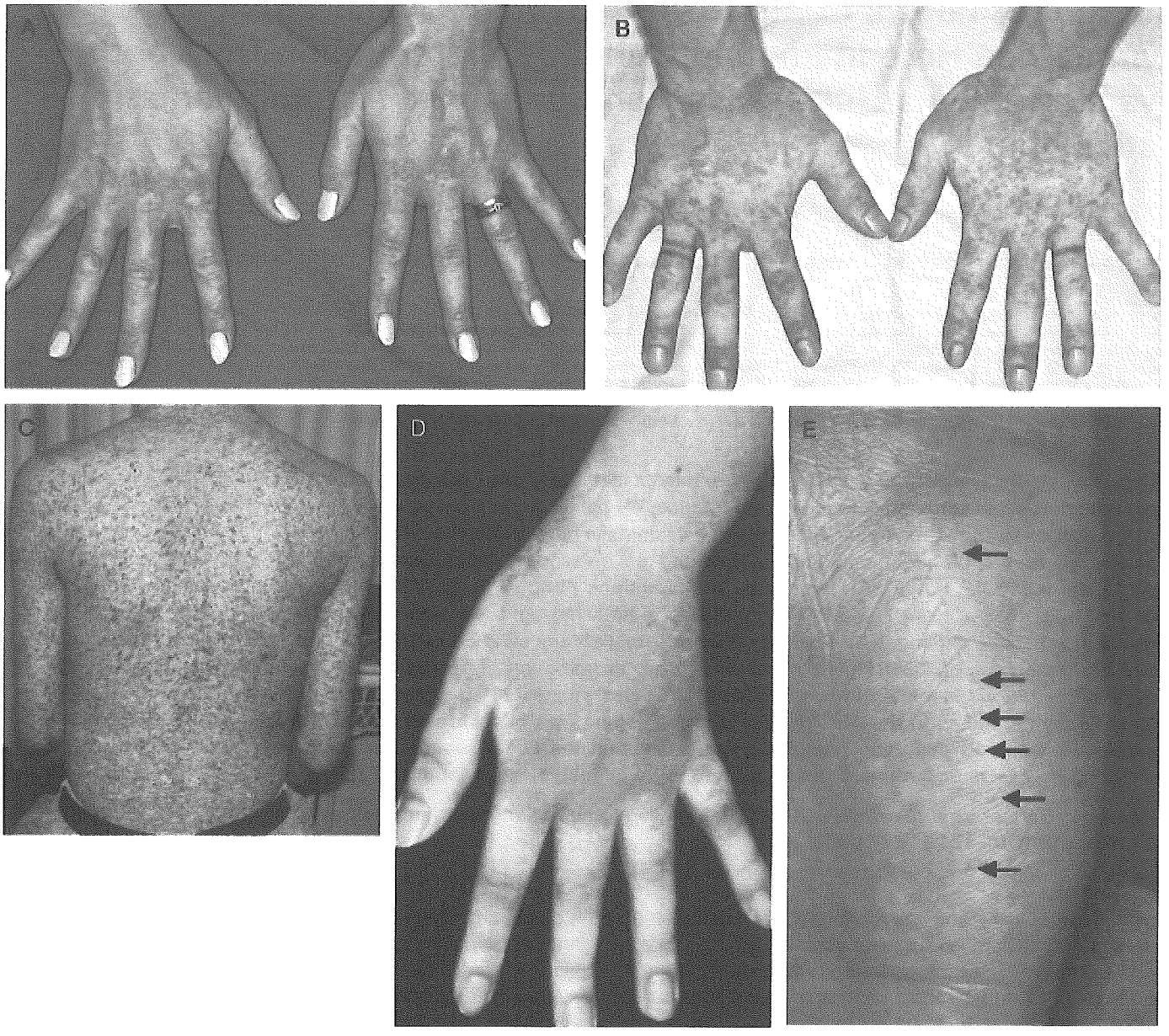

Figure 1
Clinical phenotypes of dyschromatosis symmetrica hereditaria (DSH), dyschromatosis universalis hereditaria (DUH), and acropigmentatio reticularis (AR). (*A*) Patient 3 with DSH, (*B*) patient 8 with DSH. The mixtures of hyper- and hypopigmented macules on the dorsal aspects of hands were various. The phenotype in patient 3 was faint and less severe than that in patient 8. (*C*) DUH. Mixtures of hyper- and hypopigmented macules occur all over the body. (*D*), (*E*) AR. Hyperpigmented macules distributed on the dorsal aspects of the hands and feet with no hypopigmented ones. "Pits" on the palms (*arrows*) were observed.

substrates, the editing occurs at specific sites to produce codon changes within open reading frames, whereas in others an alternative splice acceptor site is created, or modulation of mRNA stability or transport is changed by editing pre-mRNA (Maas *et al*, 2003). Loss of those functions might cause the phenotypes of DSH, although the mechanisms still remain unknown.

There are two diseases showing phenotypes so similar to DSH that they are sometimes difficult to differentiate from DSH. One of them is dyschromatosis universalis hereditaria (DUH [MIM127500]), initially described by Ichikawa and Hiraga (1933). In DUH, mixtures of hyperpigmented and hypopigmented macules occur all over the body (Fig 1*C*). By the localization of the skin lesions, the disease can be discriminated from DSH. And DUH has been thought to be distinct from DSH because they have not been found together in the same pedigree. We previously suggested (Miyamura *et al*, 2003) that DUH might have been the diagnosis in the two families in which Xing *et al* (2003) found linkage to 6q24.2–q25.2. The other disease is acropigmentatio reticularis (AR) (Kitamura *et al*, 1953), also called "reticulate acropigmentation of Kitamura" (Griffiths, 1976), which is also an autosomal dominant disease characterized by reticulate, hyperpigmented macules distributed on the dorsal aspects of the hand and feet, "pits" on the palms, and the absence of hypopigmented macules (Fig 1*D* and *E*). It is controversial whether AR is a variant of DSH. So far there has been no report on the chromosomal location or etiology of AR.

In this paper, we report 16 novel mutations in Japanese patients with DSH; these mutations help to define a func-

tionally important region in the deaminase domain. We also report that none of the three patients with DUH or the three patients with AR had any mutations in the *ADAR1* gene, supporting the notion that DSH is a distinct disease from DUH or AR. This is a report showing molecular evidence of the differences between DSH and DUH as well as AR.

Results and Discussion

Mutations of the *ADAR1* gene in patients with DSH PCR-single-strand conformation polymorphism/heteroduplex (SSCP/HD) screening and direct sequencing of the 16 patients with DSH revealed 16 novel mutations of the *ADAR1* gene (Table I). The 16 novel mutations included six missense substitutions (p.V906F, p.K1003R, p.G1007R, p.C1036S, p.S1064F, p.R1078C), two splice site mutations (IVS2+2T>G, IVS8+2T>A), six frameshift mutations (p.H216fs, p.K433fs, p.G507fs, p.P727fs, p.V955fs, p.K1201fs), and two nonsense mutations (p.R426X, p.Q600X). We examined the frequency of the six missense and the two splice site mutant alleles in the *ADAR1* gene of 114 unrelated normally pigmented Japanese subjects (228 alleles), and no mutant allele was detected. This suggested that those 8 alleles were very rare in the normal Japanese population and could be defined statistically as pathological alleles. Furthermore, in the case of a splice site mutation, IVS8+2T>A, we confirmed an aberrant splice product with RT-PCR and DNA direct sequence analysis. The result revealed that exon 8 was spliced to exon 9 with the presence of the first 80 nucleotides from intron 8, resulting in a frameshift and a truncated protein with an additional 2-amino-acid peptide. In another splice site mutation, IVS2+2T>G, we predicted that the T>G change at the second base of IVS2 might cause a similar aberrant splicing. We could not, however, obtain experimental evidence because the patient did not agree to provide an additional blood sample for the RT-PCR work. All of the six novel missense mutations identified in this study and another five missense mutations described previously (Miyamura *et al*, 2003; Li *et al*, 2004; Liu *et al*, 2004; Zhang *et al*, 2004) were

Table I. Mutations of the *ADAR1* gene in this study

Patient	Disease	Incidence	Affected individuals	Unaffected individuals	Nucleotide change[a]	Amino acid change	Exon	Mutation type
1	DSH	Familial	3	1	c.645–646insCC	p.H216fsX261	EX2	Frameshift
2	DSH	Familial	4	9	c.1276A>T	p.R426X	EX2	Nonsense
					c.1826T>C	p.F609S	EX4	Missense
3	DSH	Familial	5	11	c.1296–1297insTG	p.K433fsX433	EX2	Frameshift
4	DSH	Familial	7	5	c.1521delG	p.G507fsX509	EX2	Frameshift
5	DSH	Familial	6	9	IVS2+2T>G	Unknown	IVS2	Splice mutation
6	DSH	Familial	5	2	c.1798C>T	p.Q600X	EX4	Nonsense
7	DSH	Familial	4	15	c.2180delC	p.P727fsX792	EX6	Frameshift
8	DSH	Familial	7	13	IVS8+2T>A	p.G890fsX892	IVS8	Splice mutation
9	DSH	Sporadic	—	—	c.2716G>T	p.V906F	EX9	Missense
10	DSH	Familial	2	6	c.2865–2866delGT	p.V955fsX972	EX10	Frameshift
11	DSH	Familial	7	5	c.3008A>G	p.K1003R	EX11	Missense
12	DSH	Familial	2	10	c.3019G>A	p.G1007R	EX11	Missense
13	DSH	Sporadic	—	—	c.3107G>C	p.C1036S	EX12	Missense
					c.1752–1754delATC	p.S585del	EX3	Frameshift
14	DSH	Familial	3	10	c.3191C>T	p.S1064F	EX12	Missense
15	DSH	Familial	5	3	c.3232C>T	p.R1078C	EX13	Missense
16	DSH	Familial	8	9	c.3603delA	p.K1201fsX1203	EX15	Frameshift
17	DUH	Familial	4	6	None	None		
18	DUH	Sporadic	—	—	None	None		
19	DUH	Sporadic	—	—	None	None		
20	AR	Familial	2	1	None	None		
21	AR	Familial	4	4	None	None		
22	AR	Sporadic	—	—	None	None		

[a]GenBank Accession No. NM_001111. Position 1 is A of the translation initiation codon.
DSH, dyschromatosis symmetrica hereditica.

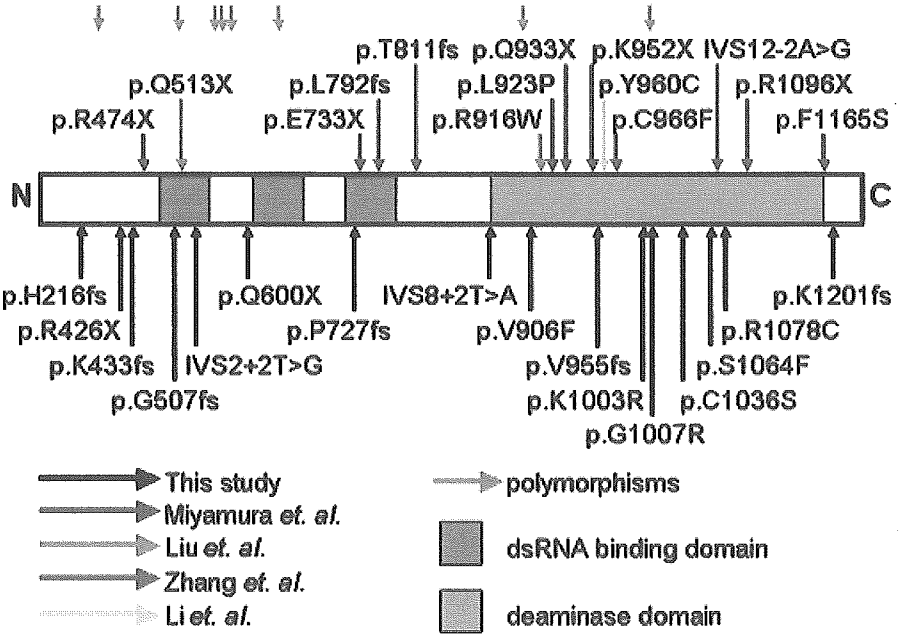

Figure 2
Mutations of the *ADAR1* gene found in patients with dyschromatosis symmetrica hereditaria. The new mutations and polymorphisms identified in this study are indicated by black and pink arrows, respectively. Blue, green, red, and yellow arrows indicate mutations reported previously. N, N-terminal; C, C-terminal.

located at amino-acid residues conserved among the zebrafish, frog, chicken, mouse, and human within the deaminase domain of the ADAR1 protein (Fig 2). These results suggested that the mutations play an important role in the confirmation of the catalytic site of the enzyme and likely influence the deaminase activity.

Patient 2 turned out to have two mutations, p.R426X and p.F609S (Table I). We examined the frequency of these two mutations among 101 of the normally pigmented Japanese subjects (202 alleles), and neither mutation was detected. Further analysis of his father with DSH showed that he also had both mutations, indicating that the two mutations must be certainly on the same allele derived from him, but not on two heterozygous alleles. Therefore, the p.F609S mutation might not give any influence in this patient because of the existence of the previous p.R426X mutation, which would lead to premature translation resulting in a truncated protein with no functional activity. And this would not be contradictory to a report that homozygosity for the *Adar1* null mutation would cause embryonic lethality in mice (Wang *et al*, 2004).

Identification of polymorphisms We identified six novel polymorphisms in the exonic or the nearby intronic sequences in the *ADAR1* gene, and the frequencies were determined for 16 patients with DSH and 113 unrelated normal Japanese subjects (Table II). Two of the exonic polymorphisms resulted in amino-acid changes (p.K384R, p.Y587C), one resulted in an in-frame mutation (p.S585del), whereas the remaining ones were silent. A three-base deletion (ATC) at c.1752–1754, which was an in-frame mutation resulting in a deletion of serine located outside of the deaminase domain, was found in one patient (patient 13) and two normally pigmented Japanese. Patient 13 was homozygous for this deletion and heterozygous for p.C1036S (Table II). The amino-acid substitution from cystein to serine at codon 1036 is a non-conserved change located within the deaminase domain, suggesting a pathological mutation. And the two normal subjects who were heterozygous for p.S585del mutant allele had no evidence for DSH. Based on these data, we concluded that the deletion of the serine codon 585 is a sequence polymorphism rather than a pathogenic mutation, although the possibility of a rare recessive allele cannot be excluded.

The relationship between the phenotype and the mutant genotype in the *ADAR1* gene We compared the clinical features among the patients with the mutations identified in the 16 cases. All of the patients had a mixture of hyper- and hypopigmented macules to various extents, which first appeared in infancy or early childhood. Some patients (e.g., patient 8, Fig 1*B*) had markedly clear macules. On the other hand, faint macules were found on the dorsal aspects of the extremities of the other patients (e.g., patient 3, Fig 1*A*). We failed, however, to find any relationship between the phenotypes and genotypes; even in the same family and pedigree among those who had the same mutation, the pattern and the degree of the skin lesions were various. There was no tendency that the phenotype in a patient who had a missense mutation or a relatively long truncation peptide might be less severe than that in a patient with an early truncation mutation. These data indicated that the phenotypes might be influenced not only by mutant genotypes in the *ADAR1* gene but also by other genes or, possibly, the patient's environment, e.g., repeated exposure to UV light on the dorsal aspects of the hands and feet.

DUH and AR We screened mutations in the *ADAR1* gene in the three patients with DUH and three patients with AR by both the SSCP/HD method and direct sequencing of all their PCR products. No mutation, however, was identified (Table I). These findings indicated that the gene causing DUH or AR should be different from *ADAR1* and that these disorders are genetically and etiologically distinct from DSH. And they also supported our previous suggestion that DSH and DUH may be two distinct diseases, that is, the

Table II. Polymorphisms detected in the *ADAR1* gene and its frequencies in Japanese patients with DSH and normally pigmented Japanese subjects

Nucleotide change	Amino acid change	Exon	Allele frequency in	
			Japanese patients with DSH	Normally pigmented Japanese subjects
c.1151G>A	p.R384K	EX2	7/24(0.29)	10/36(0.28)
c.1410A>G[a]	p.P470P (silent)	EX2	0/32(0.00)	1/36(0.03)
c.1752–1754delATC[a]	p.S585del	EX3	2/32(0.06)	2/226(0.01)
c.1760A>G[a]	p.Y587C	EX3	0/32(0.00)	2/226(0.01)
IVS3+5G>A[a]	None	IVS3	0/32(0.00)	4/226(0.02)
IVS4-20C>T[a]	None	IVS4	1/32(0.03)	1/36(0.03)
c.2682G>A	p.V894V (silent)	EX9	7/20(0.35)	64/222(0.29)
IVS11+9T>C[a]	None	IVS11	0/32(0.00)	1/36(0.03)

[a]Novel polymorphism.
DSH, dyschromatosis symmetrica hereditaria.

locus for DUH might link to chromosome 6q24.2–q25.2 whereas that for DSH links to chromosome 1q21.3 (Miyamura *et al*, 2003).

Recently, Nuber *et al* (2004) reported in an ultrastructural skin investigation of DUH patients that DUH might not be a disorder of the melanocyte number, but rather that of the melanosome synthesis rate. This is intriguing in view of reports describing that the pigment anomaly in DSH might be due to the small number of melanocytes (Hata and Yokomi, 1985), indicating that the two diseases might be caused by quite different mechanism(s) in spite of the similarity in phenotypes.

AR had sometimes been proposed to be a variant of DSH. Hyperpigmented macules, which are similar to those of DSH, distribute on the dorsal aspects of the hands and feet. The difference in clinical features from DSH is the absence of hypopigmented macules (Fig 1*D*), which are always found in DSH. "Pits" on the palms (*arrows*) are observed in AR and enable one to differentiate between DSH and AR (Fig 1*E*). Our present data indicated that AR is an entirely different disease from DSH.

ADAR1 protein is composed of 1226 amino acid residues, with a calculated molecular mass of 139 kDa (O'Connell *et al*, 1995). It catalyzes the deamination of adenosine to inosine in double-stranded RNA substrates (Bass and Weintraub, 1988; Wagner *et al*, 1989), which results in the creation of alternative splicing sites (Rueter *et al*, 1999) or alternations of codon and thus leads to functional changes in proteins. The *ADAR1* gene is expressed ubiquitously (Kim *et al*, 1994), but a few known target genes for ADAR1 are expressed in specific tissues, e.g., ionotropic glutamate receptor (Higuchi *et al*, 1993; Lomeli *et al*, 1994) and the serotonin receptor 2C subtype in the brain (Burns *et al*, 1997), and hepatitis delta virus antigen in the liver (Polson *et al*, 1996). And it was also reported that the *ADAR1* expression was increased in the spleen, thymus, and peripheral lymphocytes of endotoxin-treated mice (Yang *et al*, 2003). The target genes and the induction of the enzyme in lymphocytes, however, are unlikely to be involved in the pathogenesis of DSH. Wang *et al* recently reported that homozygosity for the *Adar1* knockout in mice caused embryonic lethality, indicating that *Adar1* was essential for life. And they further observed that fibroblasts derived from $Adar^{-/-}$ embryo were prone to apoptosis induced by serum deprivation. $Adar^{+/-}$ heterozygous mice, however, exhibited no obvious abnormalities such as skin lesions (Wang *et al*, 2004). The absence of skin lesions in the heterozygous mice may depend on differences between the two splices.

The mechanism by which mutations in *ADAR1* gene cause DSH still remains unknown. We speculate two hypotheses as follows. The first is that, when melanoblasts migrate from the neural crest to the skin during development, a greater reduction in ADAR1 activity might occur at anatomic sites distant from the neural crest. The failure of correct RNA editing may induce the differentiation of melanoblasts to hyperactive or hypoactive melanocytes, which then colonize in an irregular distribution resulting in skin lesions. The second hypothesis is that the ADAR1 activity is required for protection against stress-induced apoptosis as mentioned above (Wang *et al*, 2004). Accordingly, a greater reduction in ADAR1 activity would cause apoptosis in melanocytes at sites exposed to UV light and would result in hypopigmented macules on the back of the hands and the top of the feet. And secondarily, hyperpigmentation might occur around hypopigmented macules completing the mixture of hypo- and hyperpigmented macules. These hypotheses were based on the idea that nonsense-mediated RNA decay would occur and DSH might be caused by haploinsufficiency of the ADAR1 activity, because we failed to identify a clear relationship between the phenotypes and genotypes in this study described above. That is, there was no phenotypical difference in terms of the kind and site of the mutations. A dominant negative effect of mutant ADAR1 activity, however, could also be proposed as a mechanism as well as haploinsufficiency. Recently, homodimerization was demonstrated to be essential for the enzyme activity of the *ADAR1* encoded protein (Cho *et al*, 2003). Both the double-stranded RNA binding motif and deaminase domain were suggested to be required for the

formation of the homodimer (Cho *et al*, 2003), suggesting that DSH might be caused by a dominant negative effect (Liu *et al*, 2004). Further investigations will be needed to address this issue.

In conclusion, in this study, 16 novel mutations in the *ADAR1* gene were found in 16 Japanese patients with DSH, suggesting no founder effect in DSH patients. And this study also established the existence of apparent differences in the etiology of DSH, DUH, and AR. Identification of the genes for DUH and AR is expected.

Materials and Methods

Patients All patients were Japanese and unrelated. A total of 16 patients with DSH, three patients with DUH, and three patients with AR were included in the mutational analysis. Two, two, and one of the patients with DSH, DUH, and AR, respectively, had no family history of the disease and the families of the other patients turned out to have at least one other affected individual in each family (Table II). We screened one affected individual of each pedigree for a mutation of the *ADAR1* gene. The birthplaces of the patients were scattered around Japan, and no high incidence area for these three diseases were found. The patients originally consulted us for their skin conditions. The degree of hyper- and hypopigmentation in each patient varied from distinct to indistinct. This study was approved by the Ethics Committee of Nagoya University Graduate School of Medicine. This study was conducted according to the Declaration of Helsinki Principles. Informed written consent was obtained from each patient, or from the patient's parents in the case of children.

Mutation screening and detection Mutation analysis of the *ADAR1* gene was performed as previously described (Miyamura *et al*, 2003). Briefly, genomic DNA was extracted from peripheral blood leucocytes and used as a template for mutational screening using a PCR-based SSCP/HD analysis (Spritz *et al*, 1992). Standard PCR amplification procedures were employed, with an annealing temperature of 62°C for all primers (see Table S1). Three kinds of SSCP gels, with glycerol concentrations of 0%, 7%, and 10%, were used to elevate the sensitivity of our mutation screening system. PCR products showing aberrant patterns on SSCP were reamplified and sequenced directly to identify the mutation. In patients without any mutations detected by the SSCP/HD method, all of their PCR products were directly sequenced to identify any mutations.

The authors are grateful to the patients and the volunteers for donating blood samples. We also thank the Department of Dermatology, Tokyo Women's Medical University for introducing a patient to our project. This work was supported by grants (Grant number: 16591095, 16044221, and 16390315) from the Ministry of Education, Sports, Culture, Science, and Technology of Japan for T. Suzuki and Y. Tomita.

Supplementary Material

The following material is available from http://www.blackwellpublishing.com/products/journals/suppmat/JID/JID23732/JID23732.htm

Table S1. Primer pairs used to amplify the *ADAR1* gene exon segments.

DOI: 10.1111/j.0022-202X.2005.23732.x

Manuscript received October 1, 2004; revised form January 20, 2005; accepted for publication January 30, 2005

Address correspondence to: Tamio Suzuki, MD, PhD, Nagoya University Graduate School of Medicine, Department of Dermatology 65 Tsurumai, Showa-ku, Nagoya 466-8550, Japan. Email: tasuzuki@med.nagoya-u.ac.jp

References

Bass BL, Weintraub H: An unwinding activity that covalently modifies its double-stranded RNA substrate. Cell 55:1089–1098, 1988

Burns CM, Chu H, Rueter SM, Hutchinson LK, Canton H, Sanders-Bush E, Emeson RB: Regulation of serotonin-2C receptor G-protein coupling by RNA editing. Nature 387:303–308, 1997

Cho DS, Yang W, Lee JT, Shiekhattar R, Murray JM, Nishikura K: Requirement of dimerization for RNA editing activity of adenosine deaminase acting on RNA. J Biol Chem 278:17093–17102, 2003

Griffiths WA: Reticulate acropigmentation of Kitamura. Br J Dermatol 95: 437–443, 1976

Hata S and Yokomi I: Density of dopa-positive melanocytes in dyschromatosis symmetrica hereditaria. Dermatologica 171:27–29, 1985

He PP, He CD, Cui Y, *et al*: Refined localization of dyschromatosis symmetrica hereditaria gene to a 9.4-cM region at 1q21–22 and a literature review of 136 cases reported in China. Br J Dermatol 150:633–639, 2004

Higuchi M, Single FN, Kohler M, Sommer B, Sprengel R, Seeburg PH: RNA editing of AMPA receptor subunit GluR-B: A base-paired intron exon structure determines position and efficiency. Cell 75:1361–1370, 1993

Ichikawa T, Hiraga Y: A previously undescribed anomaly of pigmentation dyschromatosis universalis hereditaria. Jpn J Dermatol Urol 34:360–364, 1933 (in Japanese)

Kim U, Wang Y, Sanford T, Zeng Y, Nishikura K: Molecular cloning of cDNA for double-stranded RNA adenosine deaminase, a candidate enzyme for nuclear RNA editing. Proc Natl Acad Sci USA 91:11457–11461, 1994

Kitamura K, Akamatsu S, Hirokawa K: Eine besondere Form der Akropigmentation: Acropigmentatio reticularis. Hautarzt 4:152–156, 1953

Li M, Jiang YX, Liu JB, *et al*: A novel mutation of DSRAD gene in a Chinese family with gyschromatosis symmetrica hereditaria. Clin Exp Dermatol 29: 533–535, 2004

Liu Q, Liu W, Jiang L, *et al*: Novel mutations of the RNA-specific adenosine deaminase gene (DSRAD) in Chinese families with dyschromatosis symmetrica hereditaria. J Invest Dermatol 122:896–899, 2004

Lomeli H, Mosbacher J, Melcher T, *et al*: Control of kinetic properties of AMPA channels by nuclear RNA editing. Science 266:1709–1713, 1994

Maas S, Rich A, Nishikura K: A-to-I RNA editing: Recent news and residual mysteries. J Biol Chem 278:1391–1394, 2003

Miyamura Y, Suzuki T, Kono M, Inagaki K, Ito S, Suzuki N, Tomita Y: Mutations of the RNA-specific adenosine deaminase gene (DSRAD) are involved in dyschromatosis symmetrica hereditaria. Am J Hum Genet 73:693–699, 2003

Nuber UA, Tinschert S, Mundlos S, Hauber I: Dyschromatosis universalis hereditaria: Familial case and ultrastructural skin investigation. Am J Med Genet 15:261–266, 2004

O'Connell MA, Krause S, Higuchi M, Hsuan JJ, Totty NF, Jenny A, Keller W: Cloning of cDNAs encoding mammalian double-stranded RNA-specific adenosine deaminase. Mol Cell Biol 15:1389–1397, 1995

Oyama M, Shimizu H, Ohata Y, Tajima S, Nishikawa T: Dyschromatosis symmetrica hereditaria (reticulate acropigmentation of Dohi): Report of a Japanese family with the condition and a literature review of 185 cases. Br J Dermatol 140:491–496, 1999

Polson AG, Bass BL, Casey JL: RNA editing of hepatitis delta virus antigenome by dsRNA-adenine deaminase. Nature 380:454–455, 1996

Rueter SM, Dawson TR, Emeson RB: Regulation of alternative splicing by RNA editing. Nature 399:75–80, 1999

Spritz RA, Holmes SA, Ramesar R, Greenberg J, Curtis D, Beighton P: Mutations of the KIT (mast/stem cell growth factor receptor) proto-oncogene account for a continuous range of phenotypes in human piebaldism. Am J Hum Genet 51:1058–1065, 1992

Toyama I: An unknown disorder of hyperpigmentation. Jpn J Dermatol Urol 10:644, 1910 (in Japanese).

Toyama I: Dyschromatosis symmetrica hereditaria. Jpn J Dermatol Urol 29: 95–96, 1929 (in Japanese)

Wagner RW, Smith JE, Cooperman BS, Nishikura K: A double-stranded RNA unwinding activity introduces structural alterations by means of adenosine to inosine conversions in mammalian cells and *Xenopus* eggs. Proc Natl Acad Sci USA 86:2647–2651, 1989

Wang Q, Miyakoda M, Yang W, Khillan J, Stachura DL, Weiss MJ, Nishikura K: Stress-induced apoptosis associated with null mutation of ADAR1 RNA editing deaminase gene. J Biol Chem 279:4952–4961, 2004

Xing Q, Wang M, Chen X, *et al*: A gene locus responsible for dyschromatosis symmetrica hereditaria (DSH) maps to chromosome 6q242–q252. Am J Hum Genet 73:377–382, 2003

Yang J-H, Luo X, Nie Y, *et al*: Widespread inosine-containing mRNA in lymphocytes regulated by ADAR1 in response to inflammation. Immunology 109:15–23, 2003

Zhang XJ, He PP, Li M, *et al*: Seven novel mutations of the ADAR gene in Chinese families and sporadic patients with dyschromatosis symmetrica hereditaria (DSH). Hum Mutat 23:629–630, 2004

Appendix

Electronic-database information Accession numbers and URLs for data presented herein are as follows:

GenBank, http://www.ncbi.nlm.nih.gov/Genbank/ (for the cDNA of human *ADAR1* [accession number NM_001111], the genomic sequence of human *ADAR1* [accession number NT_004668])

Online Mendelian Inheritance in Man (OMIM), http://www.ncbi.nlm.nih.gov/entrez/query.fcgi?db=OMIM (for ADAR1, DSH and DUH)

dbSNP Home Page, http://www.ncbi.nlm.nih.gov/SNP/ (for ADAR1-1 [accession number rs17843863], ADAR1-2 [accession number rs17843864], ADAR1-3 [accession number rs17843870], ADAR1-4 [accession number rs17843865], ADAR1-5 [accession number rs17843866], ADAR1-6 [accession number rs17843867], ADAR1-7 [accession number rs17843868], ADAR1-8 [accession number rs17843869])

Journal of Dermatological Science (2005) 37, 145—149

ELSEVIER

Journal of Dermatological SCIENCE

www.intl.elsevierhealth.com/journals/jods

Correlation of clinical severity and ELISA indices for the NC16A domain of BP180 measured using BP180 ELISA kit in bullous pemphigoid

Yukiko Tsuji-Abe, Masashi Akiyama*, Yasuko Yamanaka, Toshiro Kikuchi, Kazuko C. Sato-Matsumura, Hiroshi Shimizu

Department of Dermatology, Hokkaido University Graduate School of Medicine, North 15, West 7, Kita-ku, Sapporo 060-8638, Japan

Received 8 September 2004; received in revised form 25 October 2004; accepted 27 October 2004

KEYWORDS
Autoantibody;
BP;
BPAG2;
Indirect immunofluorescence;
Steroid resistant

Summary

Background: Titres of circulating autoantibodies detected by indirect immunofluorescence (IIF) have been used for the diagnosis and evaluation of disease activity in bullous pemphigoid (BP). In BP, the major pathogenic epitope is known to be the non-collagenous extracellular domain (NC16A) of the 180-kDa transmembrane hemidesmosomal protein (BPAG2). Recently, an enzyme-linked immunosorbent assay (ELISA) kit using the NC16A domain recombinant protein (BP180 ELISA kit) has become commercially available to measure the quantities of pathogenic autoantibodies circulating in BP patients.
Objective: To investigate the correlation of clinical severity and ELISA indices in BP.
Methods: Fourteen patients with a typical form of BP and one refractory BP patient who died despite extensive treatment were included in this study. Antibody titres in sera from these patients were measured using BP180 ELISA kit and an analysis of ELISA indices with disease activity was performed.
Results: ELISA indices were significantly reduced after successful therapy, although IIF titres did not always show apparent correlations. In the patient with refractory BP, ELISA indices also showed a good correlation with disease course. ELISA indices measured using the BP180 ELISA kit were well correlated with the disease activity.
Conclusion: This commercially available kit more closely followed disease activities than the IIF titres. The BP ELISA system may be a useful tool to evaluate the disease activity and to assess the effectiveness of the treatment of BP.

* Corresponding author. Tel.: +81 11 716 1161x5962; fax: +81 11 706 7820.
E-mail address: akiyama@med.hokudai.ac.jp (M. Akiyama).

0923-1811/$30.00
doi:10.1016/j.jdermsci.2004.10.007

1. Introduction

Bullous pemphigoid (BP) is an autoimmune blistering disease in which patients have autoantibodies to basement membrane zone (BMZ) components. The 230-kDa intracellular hemidesmosomal protein (BPAG1) and the 180-kDa transmembrane hemidesmosomal protein (BPAG2) have been identified as autoantigens in BP. The major pathogenic epitope is known to be the non-collagenous extracellular domain (NC16A) of BPAG2 [1]. Titres of circulating autoantibodies detected by indirect immunofluorescence (IIF) tests using normal human skin substrates have been used for the diagnosis and evaluation of disease activity. The clinical usefulness of the enzyme-linked immunosorbent assay (ELISA) for the detection of circulating anti-NC16A autoantibodies in the patients with BP was recently reported [2–7]. More recently, an ELISA kit using an NC16A domain recombinant protein (Medical and Biological Laboratories Co. Ltd., Nagoya, Japan) has been made commercially available to accurately measure anti-NC16A pathogenic circulating autoantibodies in BP patients' sera. In this study, using the ELISA kit, we precisely quantified the changes in ELISA indices of 14 BP patients before treatment and after remission as well as the correlation of ELISA indices and disease activity in a refractory BP patient who died, despite extensive treatment.

2. Materials and methods

2.1. Patients and sera: typical BP patients

Twenty-eight serum samples from 14 patients with BP showing typical clinical features were included in this study. Mucosal involvement was completely absent or only slight in all the cases. Out of three cases showing negative results for BP180 ELISA before treatment, two cases had no mucosal involvement and one had very slight oral mucosal lesions. In all the patients, the diagnosis was confirmed by histopathological observation and immunofluorescence study, i.e., subepidermal blister formation was seen histopathologically and direct and indirect immunofluorescence studies revealed positive autoantibody labeling in the basement membrane zone. Indirect immunofluorescent studies using 1.0 M NaCl split-skin as a substrate revealed that the IgG deposition on the basement membrane zone was on the roof side of blister in the three cases with negative BP180 ELISA before treatment. From these findings, epidermolysis bullosa acquisita was excluded in the three cases. All patients were treated successfully with oral prednisolone therapy of 30–50 mg/day with or without azathioprine or a combination therapy using tetracycline and nicotinamide. Sera were obtained for BP180 ELISA before the treatment and after the remission.

2.2. Patients and sera: a refractory BP patient who died despite extensive treatment

Twenty-one sera samples were taken from a patient with severe BP during the disease course. A 64-year-old Japanese male showed typical clinical, histopathological and immunohistopathological features of BP. His BP symptoms did not respond to treatments including oral steroid, oral immunosuppressant, and steroid pulse therapy. The patient died after 21 months of in-patient treatment due to disseminated intravascular coagulation and multiple organ failure. As far as we were able to determine, the patient had no internal malignancy.

2.3. Scoring method for clinical severity and definition of remission

Scoring criteria for clinical severity are defined as follows: 0, no skin lesions (erythema, bullae, erosions); 1, ~20% of lesions of total skin area; 2, ~40% of lesions of total skin area; 3, ~60% of lesions of total skin area; 4, ~80% of lesions of total skin area. Clinical remission was defined as when erythema, bullae and erosions healed completely and only a low dose of oral predonisolone (<5 mg/day) or no treatment was needed to maintain this condition.

2.4. Indirect immunofluorescence (IIF) for circulating autoantibodies

Indirect immunofluorescence was performed using normal human skin as a substrate obtained from surgical operations with fully informed consent. Immunofluorescence staining was performed as previously described [8]. Fluorescence labeling was detected using an epifluorescence microscope. The highest dilution of the sera showing positive fluorescence on BMZ was adopted as the IIF titre.

2.5. ELISA for autoantibodies to NC16a domain of BPAG2 (BP180)

Concentration of IgG autoantibodies in the patients' sera directed against the NC16A domain of BPAG2 were measured using the BP180 NC16A ELISA kit following the kit's instructions. By standard, indirect

ELISA methods, 450 nm optical density values were obtained using a MICROPLATE READER (Bio-Rad Laboratories, Heracules, CA). Results were evaluated as an index value. Index value = (A_{450}<sample> − A_{450}<negative control>)/(A_{450}<positive control> − A_{450}<negative control>) × 100.

2.6. Statistical analysis

A comparison of BP180 NC16A ELISA indices before treatment and after remission was performed using an ordered logistical regression.

3. Results

3.1. BP180 ELISA indices were significantly reduced after remission, whereas IIF titres were not so closely correlated with disease severity

Sera from 14 typical BP patients were investigated. Eleven out of the fourteen patients had ELISA indices that exceeded the cut-off index value (>15) before treatment. After successful systemic therapy, the lesions were cleared in all the patients. ELISA indices of these patients after treatment were significantly reduced compared with those before the treatment ($P < 0.01$) (Fig. 1a). Mean ELISA index of the BP patients before treatment was 52.55 (range: 4.73–101.87) and the mean index after remission was 15.61 (range: 1.1–61.06). Meanwhile, the IIF titres at the same time points conversely increased in two patients (Fig. 1b). In these two patients, ELISA indices were negative both before treatment and after remission. No significant reduction in IIF titres was observed before treatment and after remission ($P > 0.05$).

3.2. Clinical disease activity was well correlated with ELISA indices during the disease course in an exceptionally severe case

We performed BP180 ELISA, 21 times during the disease course of a patient with severe disease. As shown in Fig. 2, the patient's disease relapsed twice in spite of various therapies during the disease course. The indices of BP180 ELISA were well correlated with disease activity. The mean ELISA index of this patient throughout the disease course was 144.0 (range: 25.78–225.89), which was much higher than the other untreated BP patients (mean: 52.55 (range: 4.73–101.87)).

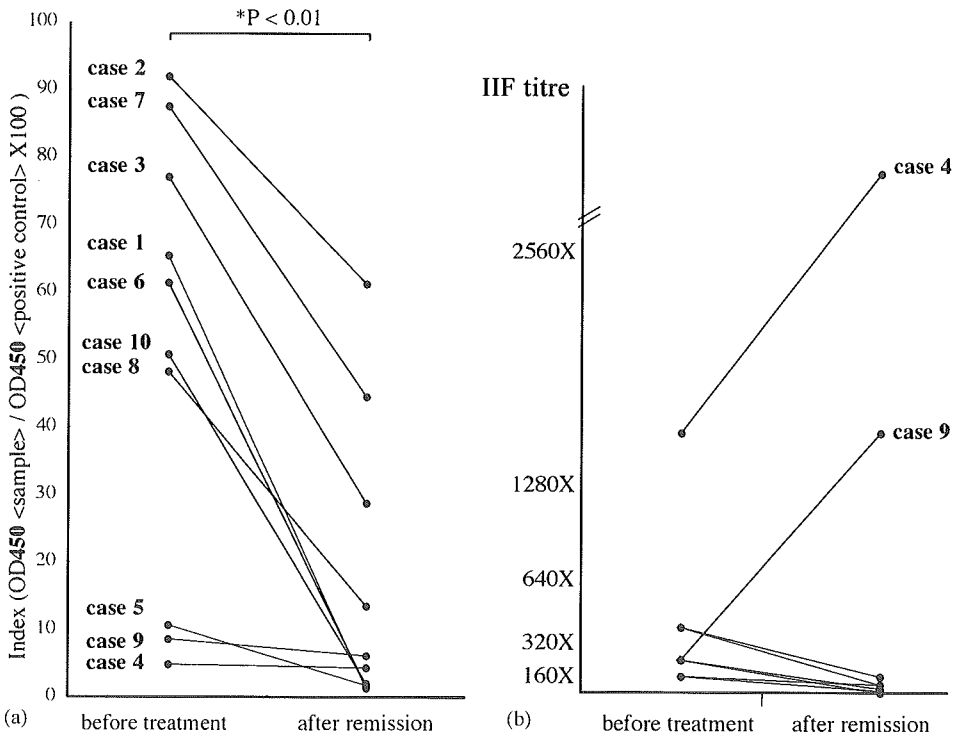

Fig. 1 Changing patterns of BPAG2 NC16A ELISA indices and IIF titres in successfully treated BP patients: (a) ELISA indices of 14 typical BP patients. Eleven out of the fourteen patients showed titres that exceeded cut-off index value (index = 15). After the successful treatment, the indices were significantly reduced ($P < 0.01$) in all the 11 cases. (b) IIF titres of the same patients. Two of 14 patients titres showed increases after remission.